

HYDROTHERMAL MODELLING FOR THE MOLTEN SALT REACTOR DESIGN OPTIMISATION

Philippe Mandin*

Laboratoire d'Electrochimie et de Chimie Analytique, UMR CNRS 7575
ENSCP, 11 rue Pierre et Marie Curie, 75231 Paris Cedex 05, France

philippe-mandin@enscp.fr

tel : +33 (0) 1 55 42 63 80

fax : +33 (0) 1 44 27 67 50

Hicham Belachgar, Alexis Nuttin, Gérard Picard,
Mailing address

belachhm@ensma.fr, nuttin@lpse.in2p3.fr, gerard-picard@enscp.fr

ABSTRACT

In this work, the concept of a molten salt reactor in term of motion and thermal design is explored . This kind of nuclear reactor uses fuel fluid which flows inside channels performed in a graphite carbon core matrix. The fluid is constituted of a molten salt mixture (here supposed 78%LiF and 22% ²³²ThF₄ with small content of ²³³U) which has to be optimized regarding neutronic constraints and core geometry. The optimum chemistry is not yet found. In the supposed core design it exists strong coupling between neutronic and hydrothermal science and also between the fluid and the carbon matrix system. The design calculation and optimization of such a system implies a rigorous mathematical formalism with a Monte Carlo calculation of the neutronic heat source and a continuous media calculation of the motion and heat transfer. This last modeling uses Navier-Stokes and energy conservation equations laws which has been solved here using the finite volume software Fluent[®]. The neutronic term appears like an energy source term which modify a lot thermodynamic and transport properties and also local motion and heat transfer. In this study, the hydrodynamic and thermal properties in a 2.5 GW thermal power project are investigated. The design rules and sensitivity analysis with parameters, such as the molten salt channels diameter or mass flow rate, are given and used.

KEYWORDS: Hydrothermal Modelling, Thorium Molten Salt Reactor

1. INTRODUCTION

The first researches concerning the molten salt reactor has been developed in the United States, at the ORNL (Oak Ridge National Laboratory). This laboratory, founded in 1943 for the plutonium preparation, is now a research place for energy and environment. The first experimental molten salt reactor (MSR) was called ARE (Aircraft Reactor Experiment) and was born in 1954. This first aircraft propulsion nuclear reactor has working hundreds hours with a 2.5 MW thermal power.

During the period ranging from 1965 to 1969, the same research center has been interested in nuclear civil energy production with the Molten Salt Reactor Experiment (MSRE). This reactor produced a 8 MW thermal power. The reactor core was graphite carbon made, pierced with numerous channels for the liquid molten salt (without thorium) flow circulation and also holes for control moderator cylinders. This experimental laboratory scale prototype has worked 5 years and has given numerous results. An industrial scale project has also early (1971-1976) interested the ORNL: the Molten Salt Breed Reactor (MSBR). This project was conceived as a thorium breeder with an exhaust plant treatment. This installation was designed to produce about 2500 MW thermal power. This

installation is shown at figure 1. Concurrent of this project was the more classical cycles, using solid combustible on the uranium/plutonium cycle for example (instead of thorium/uranium cycle for MSBR).

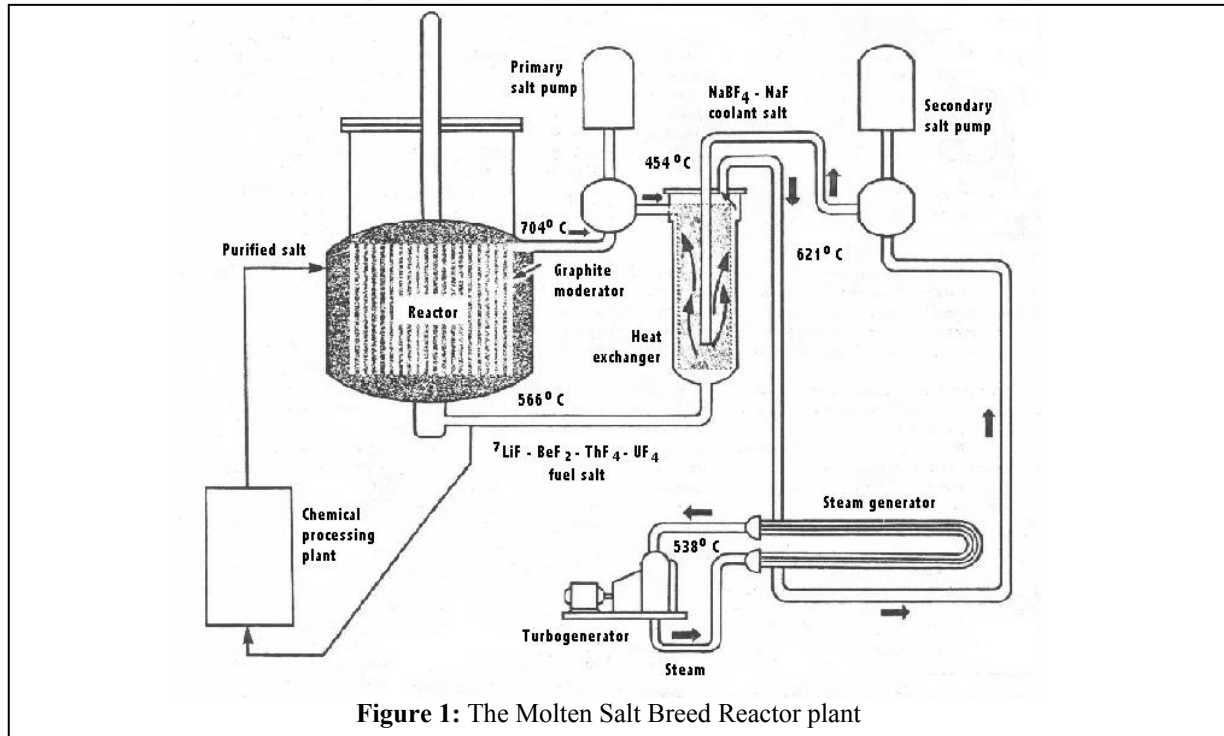


Figure 1: The Molten Salt Breed Reactor plant

The advantages of the molten salt reactor used are numerous. In this kind of reactor, the combustible is liquid and then there is no combustible melting risk as in a classical combustible reactor. Also, it is surer because the liquid is both the combustible and the cool fluid for carbon matrix. The carbon material also allows working with very high temperature. But use of molten salt as a primary fluid implies corrosion-erosion difficulties outside the core, for example in pumps or heat exchangers. The chemical composition of the liquid is the aim of numerous chemical and electrochemical studies. The goal is to define the optimal composition for neutrons, thermo-hydraulics and corrosion aspects. But for each selected chemical compositions, thermodynamical and transport liquid properties are modified. The safety has to be improved everywhere in the primary circuit, because combustible flows in the core and also outside, what is new.

2. USUAL DESIGN MACROSCOPIC STUDY

Figure 1 shows macroscopic properties of the installation. We are in this part interested in the engineer design of the primary circuit. More precisely in pressure losses and in heat exchange for this circuit.

The reactor core is a carbon matrix which is supposed to have 4.8 m in height and 4.2 m in diameter. It is constituted with carbon for 60%; the other 40% are let for the molten salt channels. Using the historically used values, the thermal power is 2500 MW.

Flow inside ducts are well known (Moody, 1944 or Sisson, 1977). Numerous works have established theoretical and empirical correlations for motion, heat or species transport, considering different hydrodynamic regimes, laminar or turbulent, established or not. In this second case, modified correlations have to be used according with Graetz theory (Bayazitoğlu Y. and Necati Özişik N., 1988). The goal of the present section is to give order of range of motion, heat and species transport between the flow and the tube. These informations are important for the corrosion-erosion modeling. It is important to know bulk and wall gradient properties in the primary circuit configurations to establish interfacial modeling.

2.1. Primary molten salt cycle

The actual primary molten salt cycle per unit can be simplified with a three elements (unit operations) cycle shown in figure 2. This can be an equivalent circuit for the all core or for a fraction (one unit) of it, like, for example, one quarter.

If the wanted total thermal power is $Power=2.5$ GW with a molten salt heating of about $\Delta T=100$ K around $T=900$ K, it is possible to calculate the total flow needed, according with $NQ= Power/(c_p\Delta T) = 2.5 \cdot 10^9/(1357 \cdot 100) = 18423 \text{ kg s}^{-1}$. For this, thermodynamical input data are needed: the density $\rho_{ms}= 3330.4 \text{ kg m}^{-3}$ and also the heat capacity $c_{p,ms}=1357 \text{ J kg}^{-1} \text{ K}^{-1}$ of the molten salt. The molten salt volume in the reactor core is $Vol_{ms} = 0.4 \cdot \pi \cdot 4.2^2 \cdot 4.8 = 26.6 \text{ m}^3$ which leads to a flowing surface $S_{ms}=Vol_{ms}/L=26.6/4.8=5.5 \text{ m}^2$ and an average density power is $p=100 \text{ MW m}^{-3}$. The average velocity should then be about $V_{ms} = NQ/(\rho S_{ms}) = 18423/(3330 \cdot 5.5) = 1 \text{ m s}^{-1}$. If a constant molten salt channel diameter $d_1=16 \text{ cm}$ is chosen, it implies a channel number $N=258$ and a mass flow rate per channel $Q=71.4 \text{ kg s}^{-1}$.

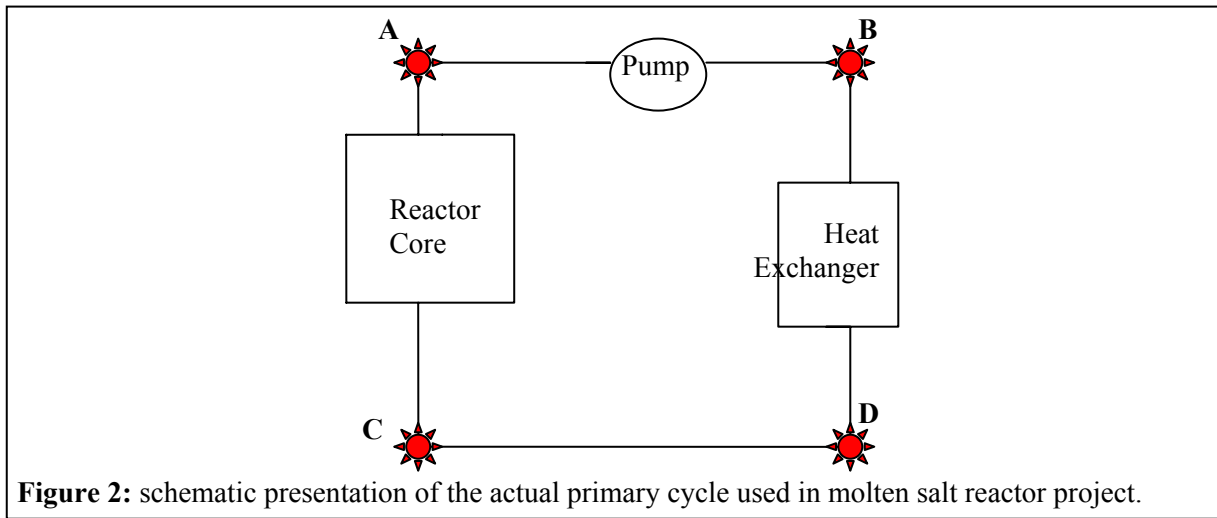


Figure 2: schematic presentation of the actual primary cycle used in molten salt reactor project.

The choice of the adapted pump to use to induced the desired flow in the reactor core need the calculation of pressure drops between and inside the three elements. The pump to choose is fixed with the mass flow rate and the pressure losses between A and B (see figure 2). For this, pressure losses inside and outside the core and heat exchanger have to be calculated. For external tubes, one of the relation (E2), (E3) or (E4), shown in paragraph below, depending with local Reynolds number and hydrodynamic regime, has to be chosen for tubes between the two elements (core and heat exchanger) for the friction coefficient f evaluation. These charge losses are usually neglected regarding charge losses in heat exchanger, and also in the core, because here, it also plays an heat exchanger role. The following parts shown the usual calculation rules for pressure drops.

2.2. Hydrodynamic properties

The more important number for hydrodynamic properties is the Reynolds number Re defined as $Re= Vd_h/\nu$, where V is the flow rate velocity (m s^{-1}), d_h is the hydraulic diameter (m) which is equal to d_1 for reactor core channels, and ν is the kinematic viscosity ($\text{m}^2 \text{ s}^{-2}$). For intensive industrial flows, the hydrodynamic regime is often turbulent established and then the Reynolds number is larger than 10^4 . In the present study, a flow regime with turbulent Reynolds number is considered.

The more interesting property for pump power design or corrosion-erosion modeling is the wall shear stress τ_p (Pa) at the tube because it rules the hydrodynamic boundary layer and then heat and mass transport boundary layers. Also because the wall shear stress is important for the mechanical effort exerted upon the steel tube, or oxide material corrosion microstructure. Its rigorous definition for an incompressible flow is:

$$\tau_p = \mu \partial V / \partial r \quad (E1)$$

The local wall shear stress is the local effort between the considered fluid packet and its neighboring. Published correlations for the friction coefficient f , allow to relate the wall shear stress with the flow Reynolds number Re . The friction coefficient is in fact the adimensional wall shear stress, according with:

$$f = 4 \tau_p / (0.5 \rho V^2) \quad (E2)$$

For perfectly smooth tubes, the Blasius law can be written:

$$f = 0.3164 Re^{-0.25} \quad (E3)$$

For rough tubes, the following implicit correlation is generally used:

$$f^{1/2} = -\log_{10}(1.255 Re^{-1} f^{0.5} + 0.269 e/d_h) \quad (E4)$$

where e is the average roughness (m).

The variation of the friction factor with Reynolds number and adimensional roughness e/d_h are now well known since Moody work in 1944. For large Reynolds number, the friction factor is almost Reynolds independent, and mostly fixed by the adimensional roughness. Then, because corrosion has a direct impact upon this adimensional roughness, for intense flows, the coupling between the flow and the corrosion properties is strong. As an evaluation, for a flow with velocity $V = 1 \text{ m s}^{-1}$, with hydraulic diameter about $d_h = 0.16 \text{ m}$, the Reynolds number is $Re = 5.3 \cdot 10^4$, and then, the minimum friction number is $f = 2 \cdot 10^{-2}$, with $\tau_p = 8.4 \text{ Pa}$ (tangential effort to be compared with the normal effort P , working pressure), which leads to hydrodynamic boundary layer thickness $\delta_h = 1.2 \text{ m m}$. These properties have been calculated using fuel salt (78% LiF – 22% ThF₄) thermophysical properties at $T = 900 \text{ K}$, used by previous authors Nuttin (2002) and Perdu (2003). These are the density ρ , the dynamic viscosity $\mu = 10^{-2} \text{ Pl}$ and the kinetic viscosity $\nu = \mu/\rho = 3 \cdot 10^{-6} \text{ m}^2 \text{ s}^{-1}$. In the present study, properties evolution with temperature are not considered.

These classical engineering tools are well known and are just here reminded for an easy fast access for future design calculations. The generalised Bernoulli law can be written:

$$E_A - E_B = (P + 0.5 \rho V^2 + \rho g z)_A - (P + 0.5 \rho V^2 + \rho g z)_B = 0.5 \rho V^2 (f L_{AB} / d_h + K) \quad (E7)$$

with subscript A and B for point A and B shown in figure 2. E is the total energy pressure (Pa) which is constituted with three components: the pressure P , the dynamic energy $0.5 \rho V^2$ and the height energy $\rho g z$ (with gravity acceleration $g = 9.81 \text{ m s}^{-2}$ and altitude z (m)). The length between A and B is written L_{AB} . K is the singular pressure drop coefficient, for example for angles in tubes: this coefficient is 1 for 90° angles. The relation (E7) allows the evaluation of pressure drops due to various causes: tube lengths (regular losses), angles (singular losses) or altitude (losses for increasing altitude). These calculations are really related with the actual final design of the primary cycle and also with core and heat exchanger properties. The mass flow rate, the tube diameter, constant or not constant, are two inputs which depends on the macroscopic circuit design. Nevertheless, a language C program has been written to have a fast evaluation of pressure drops after the choose of the heat exchanger and the core design. The pressure drops calculation in these two elements has to be carefully because in these two elements the temperature variation implies a viscosity evolution and then a rigorous calculation has to be performed.

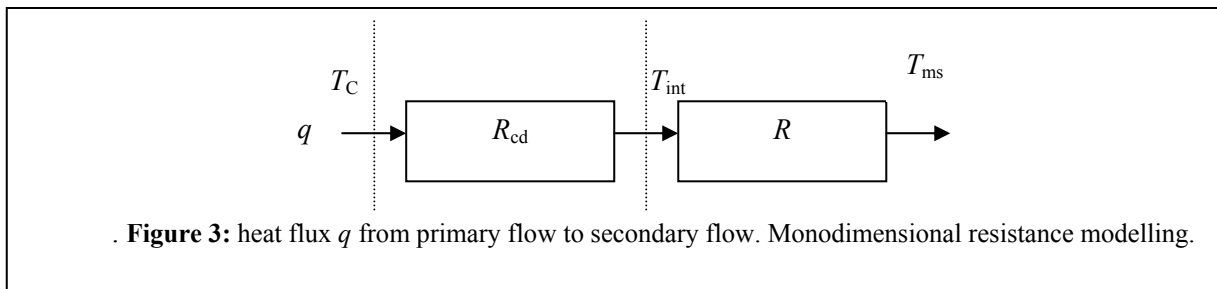
2.3. Thermal properties

Because of the molten salt flows in the core reactor, very strong thermal gradients occur which play a role for exemple upon viscosity. This because neutronic reactions imply very strong energy sources in the two core phases (carbon and molten salt) and also heat exchange between the two molten salt and carbon phases.

The local heat flux q (W m^{-2}) can be evaluated using also theoretico-empirical correlations for the Nusselt number $Nu = hd_h/\lambda$. The convective heat transfer coefficient h ($\text{W m}^{-2} \text{ K}^{-1}$) is defined using relation: $q = h(T_s - T_{\text{bulk}})$. These correlations relate the local Nusselt number Nu with the flow Reynolds number Re and the fluid Prandtl number Pr . For turbulent flows, the heat transfer rate is given using the Dittus-Boelter law (see Bayazitoğlu Y. and Necati Özişik N. 1988):

$$Nu = 0.023 Re^{0.8} Pr^c \quad (E5)$$

The heat transport is not exactly the same depending if the flow is cooled or heated with carbon phase heat exchange (respectively $c = 0.3$ or $c = 0.4$). The Prandtl number is $Pr = \mu c_p/\lambda = 11$ because the heat conduction is $\lambda_{\text{ms}} = 1.23 \text{ W m}^{-1} \text{ K}^{-1}$. The Nusselt number for the primary flow previously considered, with Reynolds number $Re = 5.3 \cdot 10^4$, leads to $Nu = 361$. Then, the heat exchange coefficient between molten salt and carbon is about $h = 2.78 \text{ kW m}^{-2} \text{ K}^{-1}$ and the thermal boundary layer thickness is $\delta_t = d_h/Nu = 4.4 \cdot 10^{-4} \text{ m}$.



The calculation of the intensive heat flux q flowing from the hot phase (generally carbon phase at temperature T_c) to the cold phase (molten salt a temperature T_{ms}), need the knowledge of the interface temperature T_{int} . This unknown is usually evaluated using a mono dimensional thermal resistance model if the shell conduction along the carbon matrix is neglected. In this modelling, two thermal resistances have to be introduced: one for the solid phase conduction R_{cd} (supposed the hotter in figure 3 scheme) and one for convective transport in molten salt. Figure 3 gives a scheme of the supposed equivalent thermal flow.

Under this modelling assumptions, it can be written for the convecto-diffusive heat flux expression:

$$q = (T_c - T_{int})/R_{cd} = (T_{int} - T_{ms})/R = (T_c - T_{ms})/R_{eq} \quad (E6)$$

with the equivalent thermal resistance ($m^2 K W^{-1}$): $R_{eq} = R + R_{cd}$

The conductive thermal resistance is $R_{cd} = d_2 \ln(d_2/d_1)/(2 \lambda_c)$, choosing the interface as the arbitrary reference surface; $d_1 = d_h$ (the molten salt channel diameter) and $d_2 = d_1 + \text{carbon phase thickness}$ between two channels. The carbon density is $\rho_c = 1843 \text{ kg m}^{-3}$, the heat capacity is $c_{pc} = 1760 \text{ J kg}^{-1} \text{ K}^{-1}$ and the conduction coefficient is $\lambda_c = 31.2 \text{ W m}^{-1} \text{ K}^{-1}$. The convective thermal resistance at the molten salt-carbon interface is: $R = 1/h$. As it can be seen, the local thermal flux q varies along the molten salt channels.

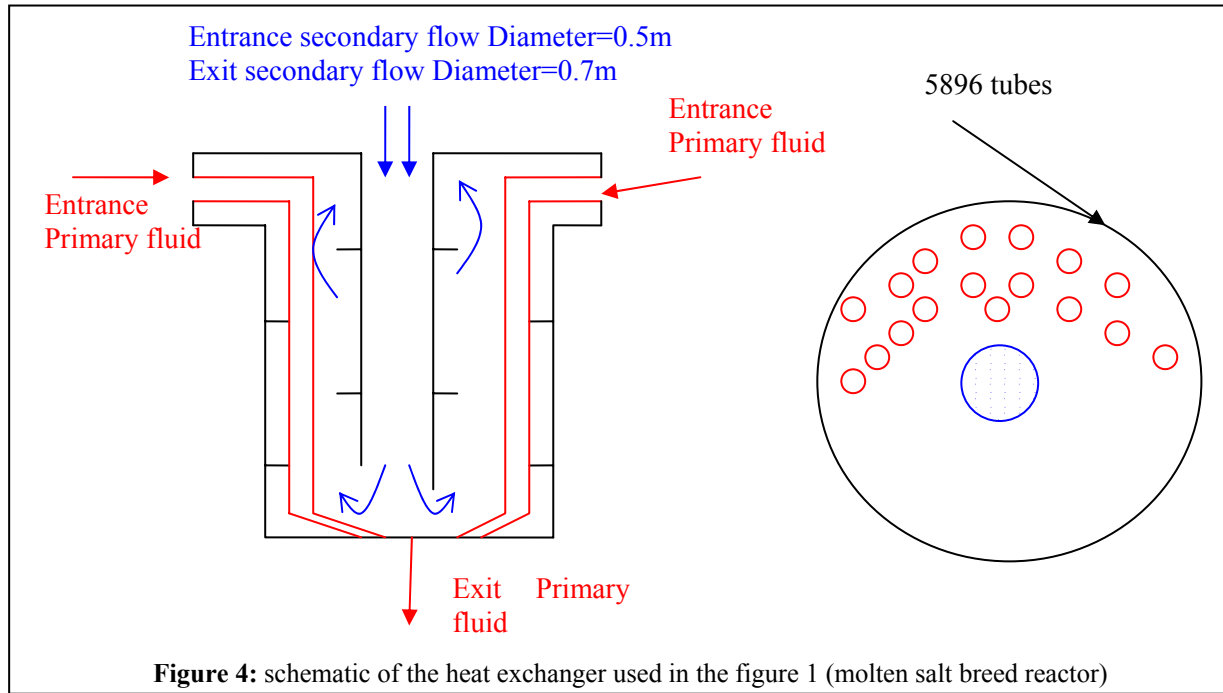
2.4. Application : heat exchanger properties

The primary flow wins heat in the reactor core due to the neutronic energy source and also because the carbon is hotter than the molten salt as it will be show. This energy is used in the heat exchanger: the heat is taken from the primary molten salt flow and is given to the secondary flow. In the present study, it has been supposed the same characteristics for the heat exchanger as these accepted for the historical MSBR.

In this historical process, the heat exchanger uses a classical counter flow configuration (see figure 4). The molten salt flows through 5896 tubes with length 6.8 m and internal and external diameters respectively equal to 7.75 mm and 9.53 mm. If one quarter of the total fuel mass flow rate is considered (4600 kg s^{-1}), the fuel mass flow rate in each tube is simply: 0.78 kg s^{-1} . The primary velocity is then 5 m s^{-1} , the Reynolds number is 12800, the Nusselt number is 91 and the heat exchange is $h = 14470 \text{ W m}^{-2} \text{ K}^{-1}$. The knowledge of the global heat transfer is not sufficient for the present study. An evaluation of the pressure losses in the primary flow has been done using the Blasius law. The friction factor is $f = 2.9 \cdot 10^{-2}$ which leads to a pressure drop $\Delta P_{\text{heat exchanger}} = 10.6 \text{ Bars}$. The actual drop is smaller because the primary flow decrease its altitude z in the heat exchanger ($\Delta z = 6.8 \text{ m}$) and then the help from gravity field is $\Delta P_{\text{gravity}} = \rho g \Delta z = 2.2 \text{ Bars}$. The actual pressure losses in heat exchanger should then be order $\Delta P_{\text{heat exchanger}} = 8.4 \text{ Bars}$.

The secondary fluid (7LiF – BeF₂ at 900 K) is supposed here to have the following physical properties: the heat capacity $c_p = 1507 \text{ J kg}^{-1} \text{ K}^{-1}$, the heat conduction $\lambda = 0.398 \text{ W m}^{-1} \text{ K}^{-1}$, the dynamic viscosity $\mu = 1.4 \cdot 10^{-3} \text{ Pl}$ and the density $\rho = 1870.4 \text{ Kg m}^{-3}$. The secondary flow historically enter the heat exchanger at $454 \text{ }^\circ\text{C}$ and exit at $621 \text{ }^\circ\text{C}$ (see figure 1). The secondary mass flow rate should then be 2480 kg s^{-1} in each of the four heat exchangers.

The temperature evolution along the flow direction is hardly non linear and the global heat exchange can't be evaluated with sufficient accuracy with a simple thermal resistance modelling. The temperature change also implies a viscosity change and then changes in pressure losses and heat transfer. It is the reason why a more rigorous calculation has been decided for the reactor core where thermal gradients, due to nuclear energy source, are very strong. This more rigorous calculation no longer used classical empirical correlations previously remind. These numerical calculations have used the computational fluid dynamic software Fluent[®]. The numerical strategy used is now presented.



3. NUMERICAL CALCULATION OF THE REACTOR CORE PROPERTIES

3.1. Navier-Stokes fluid flow modelling

For an incompressible fluid flow, the supposed stationary velocity field in the electrochemical cell must obey both the continuity equation (E8) and the Navier-Stokes equation (E9) with their appropriate boundary conditions.

$$\text{Continuity equation:} \quad \text{div}(\rho \mathbf{V}) = 0 \quad (\text{E8})$$

$$\text{Navier-Stokes equation:} \quad \rho \mathbf{V} \mathbf{grad} \mathbf{V} = \mathbf{div} \boldsymbol{\tau} - \mathbf{grad} P + \rho \mathbf{g} \quad (\text{E9})$$

In these equations, ρ is the density (kg m^{-3}), \mathbf{V} is the local velocity flow vector (m s^{-1}), $\boldsymbol{\tau}$ is the shear stress tensor (Pa), P is the local pressure (Pa) and \mathbf{g} the gravity acceleration vector (m s^{-2}).

In reactor cores or heat exchanger tubes, the flow can be supposed mono component according with $\mathbf{V} = V \mathbf{e}_z$ if z is the flow direction. The previous equations then simplifies a lot.

These two equations have to be completed with the energy equation to calculate the bidimensional or tridimensional temperature field evolution in the reactor core (in both the solid carbon phase and molten salt phase):

$$\text{Energy equation:} \quad \rho c_p \mathbf{V} \mathbf{grad} T = \mathbf{div} (\lambda \mathbf{grad} T) + p \quad (\text{E10})$$

With c_p the heat capacity ($\text{J kg}^{-1} \text{K}^{-1}$), λ the heat conduction coefficient ($\text{W m}^{-1} \text{K}^{-1}$) and p the source term (W m^{-3}). This source term is due to the energy given to both the solid and fluid phases due to the nuclear reaction. It needs to be calculated using a second software not considered here, using Monte Carlo neutronic calculations for a given temperature (phD thesis of Nuttin. A., 2002, and Perdu. F., 2003).

These equations are the equations used for laminar regime. When turbulent regimes occur the previous equations has to be modified, taking into account the increase of the transport coefficients due to vortex and also source terms for motion and energy. To illustrate, in the turbulent flow, the flow velocity and temperature is no longer constant with time: it is for each considered point an average and a standard deviation, due to the vortex. For example, local velocity V can be written: $V = V_{\text{average}} + V'$, with V' the velocity fluctuation, according with the Reynolds rules. Because the Navier Stokes equation are not linear, this decomposition leads to non linear unknown like V'^2 or $V' T'$. These unknowns need additional equations. In the present work, it has been used the classical k- ϵ turbulent flow modeling which is known to leads to good results (comparing with experimental measurements) for pressure drops and heat exchanges in ducts. For more precisions concerning turbulent regimes modeling, one can see the Bird book or Fluent[®] userguides.

3.2. Numerical Strategy

The following chosen equations (E8), (E9) and (E10) in their laminar or turbulent form, have to be solved numerically. The chosen method in the present work is the finite volume method used in the Fluent[®] software. The numerical strategy used is now presented.

3.2.1. Meshing and finite volumes method

All numerical methods of solving presented non linear differential equations need the discretisation of the calculation domain, also called the domain meshing. The numerical tool used here is the Gambit[®] software. This domain, for example one duct and its associated carbon matrix taken in the reactor core, can often be described using a bidimensional domain (z ; r), using the classical axisymetrical assumption. In the present reactor core study, it is demonstrated (Perdu or Nuttin) that the axisymetrical assumption can't be used, essentially because the neutronic energy source term is actually position and phase dependent. So, the rigorous calculation should be finally three dimensional as it will be shown at the end of the present work. The considered tube length is 4.80 m.

First, an accurate calculation needs to use sufficiently thin meshing cells particularly at walls or interfaces (between carbon and molten salt phases) regarding the motion and thermal boundary layers thicknesses (see figure 5). These thicknesses are evaluated using correlations and laws given in the second part of this work (part 2.1. for motion and 2.2. for temperature).

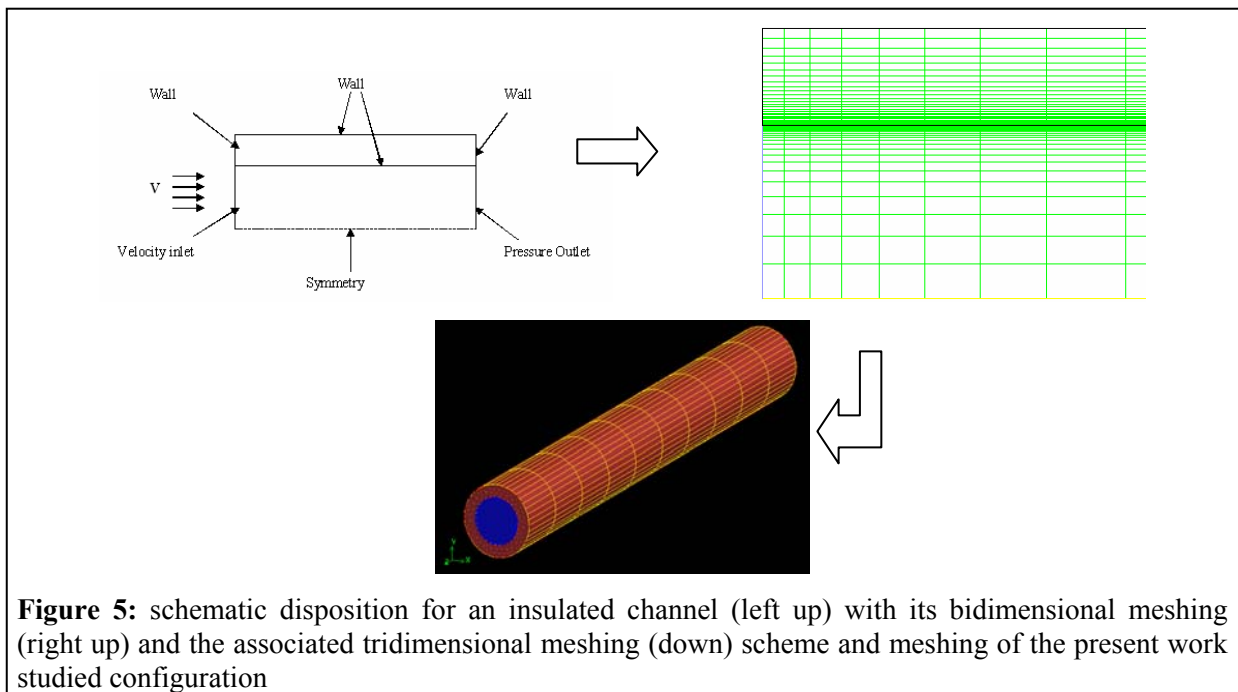


Figure 5: schematic disposition for an insulated channel (left up) with its bidimensional meshing (right up) and the associated tridimensional meshing (down) scheme and meshing of the present work studied configuration

These simplified geometrical configurations have been first used and studied to validate the meshing used. After this validation step, a rigorous three dimensional meshing and calculation of the reactor core has been performed which will be present in last results part.

Once the domain meshing is chosen, differential equations are discretised using the finite volume method of Patankar (1984). In the present study, the segregated algorithm has been used for the equations calculation. The second order scheme has been chosen for diffusive terms and the power law scheme for convective term. The velocity-pressure coupling has been solved the corrected Simple algorithm of Patankar. The energy source term has not need linearization. All these options were usable in the numerica software Fluent[®].

3.2.2. validation cases

For both laminar and turbulent regimes it has been evaluated the minimum meshing needed to have a good accordance between experimental correlation presented in part 2 or with analytical results.

Laminar validation

An arbitrary Reynolds number $Re=70$ has been chosen to illustrate the validation procedure. The molten salt channel diameter investigated is $d_h=d_1=0.16$ m. Then, according with physical properties already given, the fluid velocity and mass flow rate in each channel are respectively 1.3 mm s^{-1} and 87

g s^{-1} . Comparison with theoretical establishment lengths, motion and heat transfer is good as shown in table 1. The hydrodynamic establishment length is classically used as validation test.

It is defined as:

$$L_{\text{hydro}} = 0.056 Re d_h \quad (\text{E11})$$

	Theoretical	Numerical	Validation
Hydrodynamic length	0.62 m	0.57 m	⊙ 8 %
Average Nusselt	4.8	4.98	⊙ 3.7 %
Local Nusselt	3.8	3.75	⊙ 1.3 %
Pressure losses	$7.725 \cdot 10^{-2}$ Pa	$7.926 \cdot 10^{-2}$ Pa	⊙ 2.6 %
Friction coefficient	0.9293	0,9285	⊙ 0.86 % ₀

Table 1: Numerical calculations validation for laminar regime. Comparison with theoretical calculations

Turbulent validation

A turbulent flow with $Re=8 \cdot 10^4$ and $d_h = 0.16$ m has been considered here as an illustrating example. In this case the molten salt flow velocity and mass flow rate are respectively 1.5 m s^{-1} and 100.5 kg s^{-1} . It is a larger mass flow rate than this used in part 2 to allow the sensitivity analysis of hydrodynamic regime and to ensure the meshing validation for a more demanding case. To obtain turbulent established properties a first calculation has been made with a long tube. The output profile has been used as the input profile for the reactor core channel with length 4.8 m.

The obtained results are shown in table 2. They exhibit a correct agreement (about 10%) between the theoretical values and the numerical results obtained with the chosen mesh. The used mesh was 6240 cells (see figure 5, up right). It should have been possible to obtain better accordance using a thinner mesh, particularly near wall and at the entrance. But, because future calculations will be three dimensional, it has been chosen to minimise the cost of a one channel calculation.

	Theoretical	Numerical	Validation
Average Nusselt	502	548	⊙ 9.2%
Pressure losses	2163 Pa	2025 Pa	⊙ 6.4%
Friction coefficient	0.0192	0,02125	⊙ 10.7%

Table 2: Numerical calculations validation for turbulent regime. Comparison with theoretical calculations

Homogeneous energy source term for molten salt

The previous turbulent case is considered here again with a constant source term in the molten salt phase. The present part considers the same one channel domain with the two phases (molten salt and carbon) with the two already defined dimensions d_1 and d_2 (see figure 6). In this part, the nuclear energy source term is supposed to be homogeneous, only in the molten salt phase, according with $p = 130 \text{ MW m}^{-3}$. For a molten salt channel with length 4.8 m and 0.16 m diameter, it leads to 12.5 MW. The waiting exit temperature is then $T_{\text{ms,entrance}} + 92 \text{ K}$. Figure 6 allows a better understanding of the configuration. For more explanations, the part 2 concerning heat transfer calculation rules can be used.

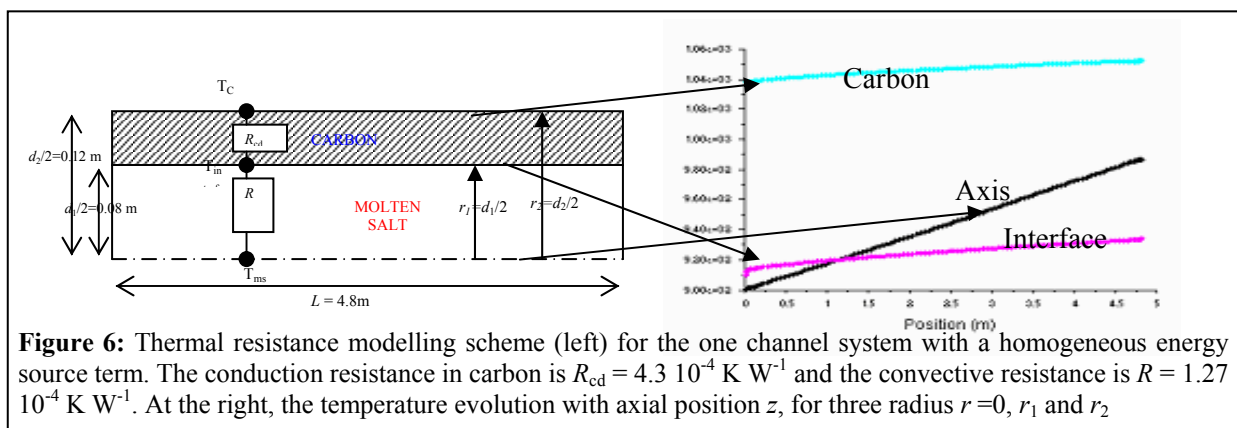
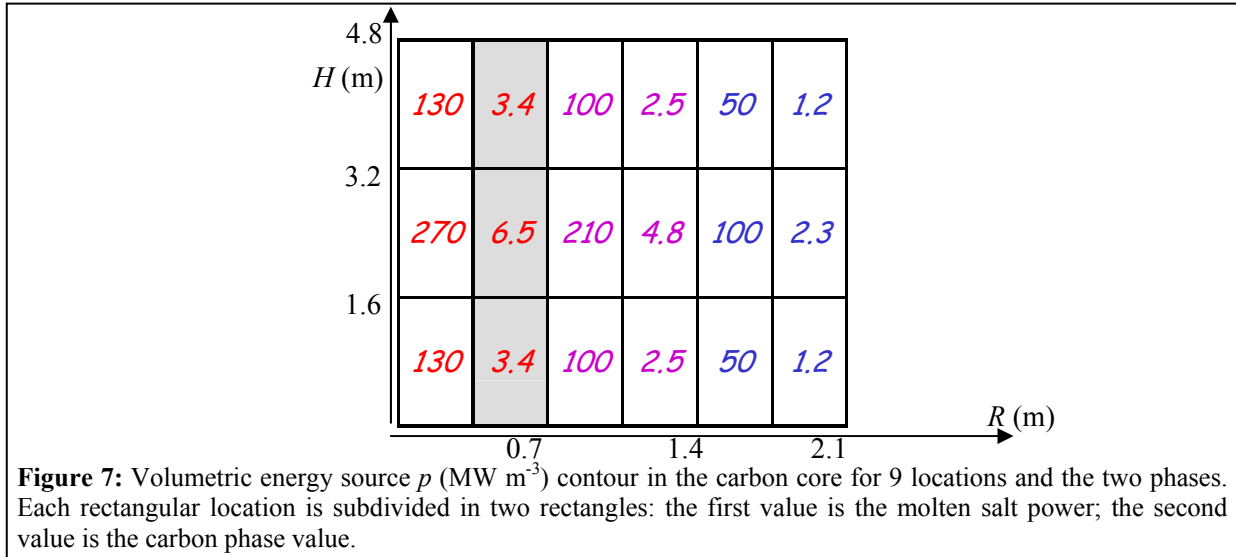


Figure 6: Thermal resistance modelling scheme (left) for the one channel system with a homogeneous energy source term. The conduction resistance in carbon is $R_{cd} = 4.3 \cdot 10^{-4} \text{ K W}^{-1}$ and the convective resistance is $R = 1.27 \cdot 10^{-4} \text{ K W}^{-1}$. At the right, the temperature evolution with axial position z , for three radius $r=0, r_1$ and r_2

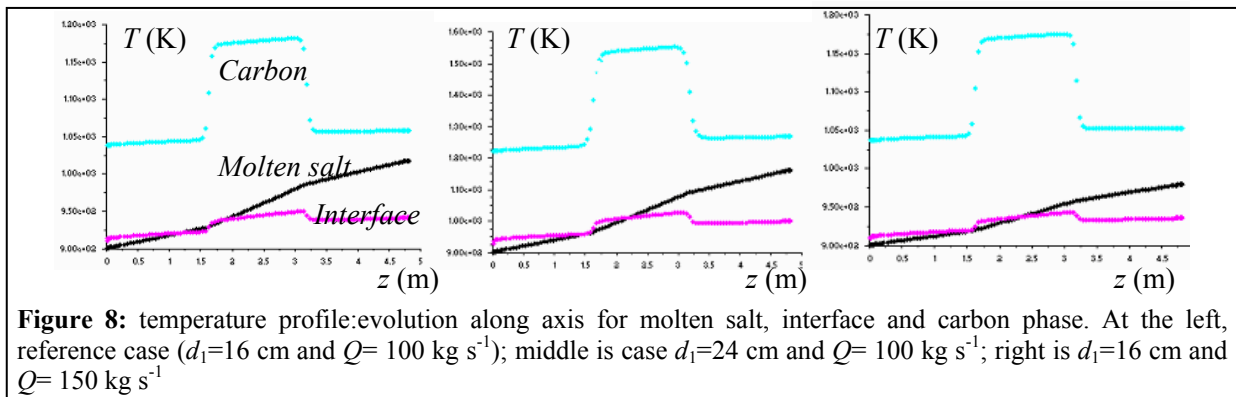
As it can be seen in figure 6, the temperature increase in the molten phase channel is 86 K which value is in good accord with the theoretical value 92 K.

3.3. Temperature profiles for one insulated axial channel

Neutronic calculations using Monte Carlo algorithms have been made (Perdu and Nuttin) to access the local energy power p (in MW m^{-3}) in the carbon core. The carbon core (2.1m radius, 4.8m height) is subdivided in 3 radial regions and 3 axial regions for both phases. The power meshing is coarser than the hydrothermal meshing: it only defines 9 locations. The values obtained for the all carbon core are shown in figure 7 for the two molten salt and carbon phases (first column: molten salt; second column: solid carbon). The total power is 2500 MW thermal.



The calculation of the bi or three dimensional character will be investigated in the last paragraph. In the present paragraph, only one insulated channel near core axis is considered. The calculation of its properties need the two first columns data which are associated to the reactor core axis power evolution for the molten salt and carbon.



Temperature (K)	$d_1=8$ $Q=50$	$d_1=8$ $Q=100$	$d_1=8$ $Q=150$	$d_1=16$ $Q=50$	$d_1=16$ $Q=100$	$d_1=16$ $Q=150$	$d_1=24$ $Q=50$	$d_1=24$ $Q=100$	$d_1=24$ $Q=150$
T_{ms} (K) entrance	900	900	900	900	900	900	900	900	900
T_{ms} (K) exit	959	929	920	1134	1017	979	1414	1159	1074
T_{in} (K) $z=0$	903	902	902	911	910	908	928	926	921
T_{in} (K) $z=4.8$ m	915	910	909	947	941	935	1000	999	979
T_C (K) $z=0$	935	934	933	1040	1038	1036	1221	1220	1211
T_C (K) $z=4.8$ m	943	938	938	1063	1057	1052	1265	1266	1246
Heat flux at interface (kW)	141.6	142.2	144.1	576.0	579.4	580.9	130.3	131.5	131.6

Table 3: One channel temperatures evolution for radius 0, 0.08 and 0.12 m and for axial position $z=0$ and 4.8 m

Sensitivity analysis has been performed with the design parameters such as the molten salt channel diameter d_1 (cm) and the molten salt mass flow rate Q (kg m^{-3}). The design of reactor must agree with the imposed condition: the molten salt volume fraction for the all reactor core must be 40% for a carbon matrix of 4.2 m diameter per 4.8 m height. Then the following relation can be written:

$$\text{Carbon Volume / Molten salt volume} = (d_2^2 - d_1^2)/d_1^2 = 60/40 \quad (\text{E12})$$

Which leads to : $d_2 = 1.58 d_1$

The estimation of the core, molten salt channels number N is: $N = 0.4 \text{ Core volume} / \text{channel volume}$

The arbitrary reference case with mass flow rate $Q=100 \text{ kg s}^{-1}$ (Reynolds number $Re = 8 \cdot 10^4$) and channel diameter $d_1=16 \text{ cm}$ leads to results shown at table 3 and figure 8.

As seen in figure 8 left, the molten salt temperature is a little smaller or equal than the interface temperature for the first half channel length. Its temperature is always smaller than the carbon temperature. Table 3 shows the temperature value for $z=0$ and 4.8 m, for the three considered radius $r=0, 8$ and 12 cm which corresponds respectively to molten salt, interface and carbon. The total heat flux transferred from carbon to molten salt is given in the last line. If the temperature increase due to convecto-diffusive transfer is estimated using the formulation $\Delta T = \text{Energy}/(Qc_p) = 4 \text{ K}$! As it can be understood, the temperature increase is mostly due to the neutronic source term. This calculation shows the good validity of a lonely channel calculation.

Table 4 shows the evolution of diameter d_2 , Reynolds Re and channel number N with parameters diameter d_1 and mass flow rate per channel Q .

d_1 (cm)	8			d_1 (cm)	16			d_1 (cm)	24		
Q	d_2 (cm)	Reynolds	N	Q	d_2 (cm)	Reynolds	N	Q	d_2 (cm)	Reynolds	N
50	12.6	79600	1050	50	25.3	39800	262	50	37.9	26500	117
100	12.6	159000	1050	100	25.3	79600	262	100	37.9	53100	117
150	12.6	239000	1050	150	25.3	119000	262	150	37.9	79600	117

Table 4: Evolution of diameter d_2 , Reynolds Re and channel number N with parameters diameter d_1 and mass flow rate per channel Q

3.4. Temperature field using a three dimensional modelling

The reactor core is actually constituted with hexagonal waffle shape carbon matrix. Figure 9 gives a scheme of the historical MSBR core reactor (left). At the figure 9 center, the waffle geometry is illustrated with the molten salt channel at center with its carbon crown. In the arbitrary reference case ($d_1=16 \text{ cm}$ and $Q=100 \text{ kg s}^{-1}$), there is about 262 channels. It has been decided to have a three dimensional simulation of the thermal properties in one tenth of the total carbon matrix. For this core fraction, about 26 channels have to be considered. A meshing example with about 100000 cells is shown in figure 9 at right.

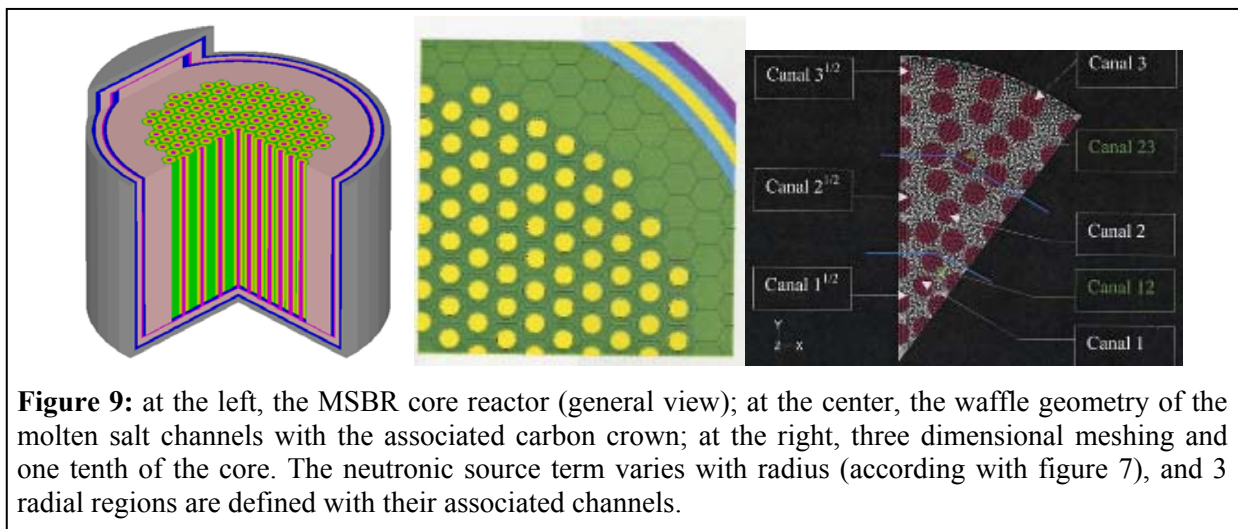


Figure 9: at the left, the MSBR core reactor (general view); at the center, the waffle geometry of the molten salt channels with the associated carbon crown; at the right, three dimensional meshing and one tenth of the core. The neutronic source term varies with radius (according with figure 7), and 3 radial regions are defined with their associated channels.

As already shown in figure 7, the neutronic energy source term varies with axial and radial position and also with phase, molten salt or carbon. Figure 9 right shows the definition of 5 channels names according with the radial variation of energy source. Channels called "1" are channels near axis ($0 < r < 0.7$ m) with the associated source term (see figure 7). Channels called 2 or 3 are also associated respectively to source term values of the second ($0.7 < r < 1.4$ m) and third ($1.4 < r < 2.1$ m) radial regions. Channels called 12 and 23 are channels at interface respectively between regions 1 and 2, and regions 2 and 3. One important obligation for the core design is to have a maximum molten salt temperature increase of about 100 K for all channels. The homogeneity of the temperature is a great wanted quality, and this for all channels (regions 1, 2 or 3). Because the neutronic source term is maximum near axis and decreases with radius, the mass flow rate should be maximum near axis and minimum at periphery. Two ways are possible: to have a non constant channel diameter, depending with considered region or to have a non constant molten salt velocity profile. This second working hypothesis has been chosen here. The inferior plenum which ensures the dispatching for molten salt has not been calculated in the present study. Three arbitrary chosen mass flow rate profiles hypothesis are explored here with a constant channel diameter $d_1=16$ cm.

Channel region	1	12	2	23	3
V_1 (m s ⁻¹)	2.4	2	1.6	1.2	0.8
ΔT_1 (K)	78	79	91	74	89
V_2 (m s ⁻¹)	2	1.6	1.2	0.5	0.5
ΔT_2 (K)	93	99	122	110	143
V_3 (m s ⁻¹)	1.8	1.6	1.5	0.7	0.7
ΔT_3 (K)	104	99	98	98	104
Q_3 (kg s ⁻¹)	119	106	99.3	46.3	46.3
Φ_3 (kW)	332.5	332.6	424.3	248.8	282.3

Table 5: Temperature drops and heat exchange Φ for molten salt depending with the channel region (1, 12, 2, 23 or 3) and with velocity (or mass flow rate Q) feeding profile. Three velocity profiles, decreasing with radius are evaluated with three dimensional thermal calculations.

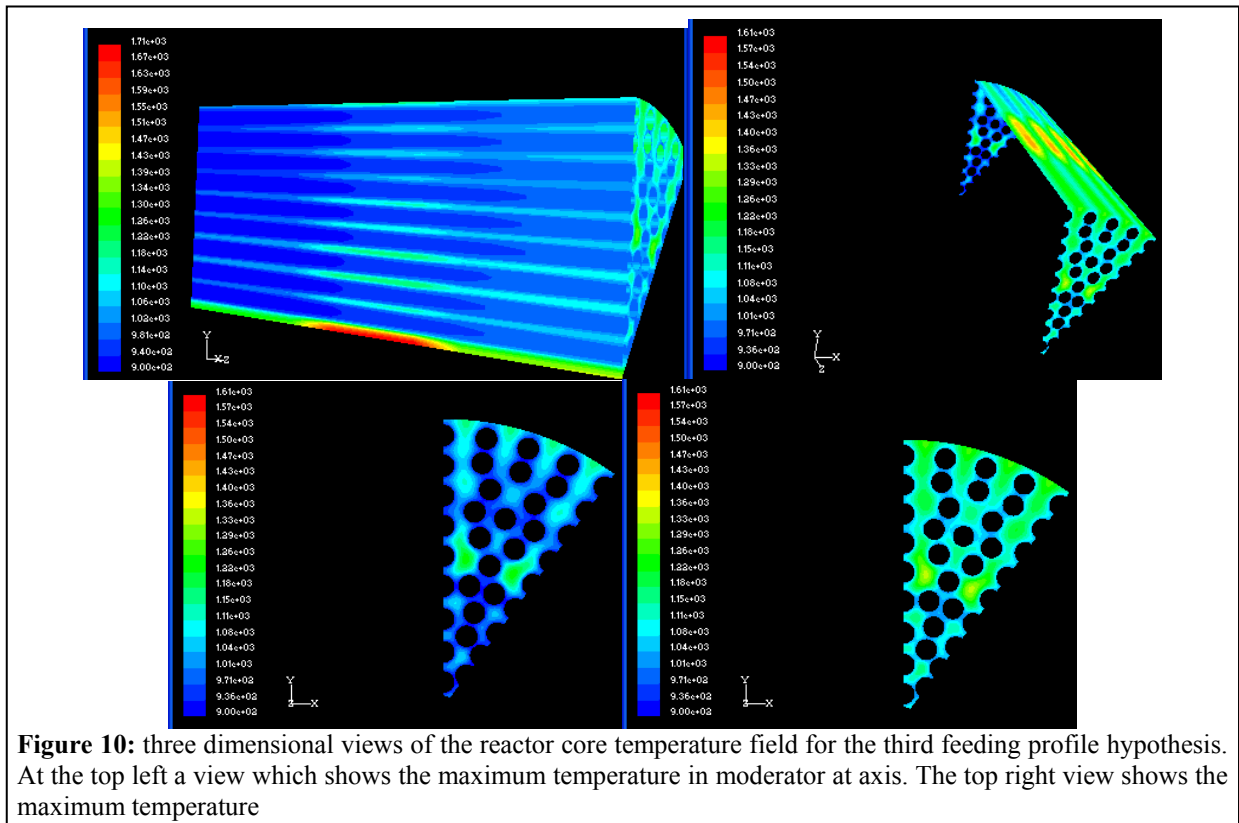


Table 5 gives three dimensional thermal calculation results for various channel feeding profiles hypothesis. The first profile hypothesis leads to smaller temperature increases than the 100 K target for obeying the total thermal power wanted. The temperature increase homogeneity is also quite bad (about 20% for an average temperature increase 85 K). The second profile hypothesis leads to an average increase 113 K with a bad homogeneity (44%). The third explored hypothesis was the better: the average temperature increase is 101 K for an homogeneity 6%. This hypothesis leads to a maximum temperature at axis 1710 K (moderator). The average temperature for carbon, molten salt and moderator is respectively 1126 K, 955 K and 1343 K. The maximum temperature for carbon phase is found at periphery with about 1610 K. Table 5 also shows in its last lines the mass flow rate \dot{Q} and the heat exchange Φ per channel.

Last figure 10 shows three dimensional views of the temperature field in the reactor core.

The calculations show a large sensitivity with geometrical disposition of channels, which, in the present study has been supposed random.

4. CONCLUSIONS

The fourth generation of nuclear plant are nowadays studied to ensure the future energetic needs of human being. Among the numerous project, the thorium molten salt reactor seems to be an interesting choice, mostly characterized with the choice of a molten salt with two roles: generator and heat transfer fluid. This concept of reactor was originally considered in the USA. The Oak Ridge laboratory has first achieved a 8 MW thermal non breed thorium prototype and has projected a more powerful project, the MSBR. Our work is related to this second project in a new frame. Calculations rules for engineering design have first be recalled. They have been applied in a second time to have pump and heat exchanger capacities estimations for the primary circuit. A more advanced thermo-hydrodynamical modeling have then be used for the reactor core properties calculation. The present work gives an estimation of thermal gradients in the carbon matrix and also in molten salt. It has also estimated consequences of feeding profiles upon core reactor properties. Safety properties should also be calculated early in the core design work, for example with unsteady calculations. For example, it is known that thermal inertia of molten salt and carbon are quite different and to be taken into account. Also, the inferior plenum which ensures the molten salt distribution has not been calculated here. In fact, it is really difficult to have more advanced modeling now because numerous freedom degrees for the cycle stay to fix, and particularly the molten salt composition which could be the presented binary salt but also could have a ternary or quaternary composition. However, because molten salt chemistry properties are very dependent with temperature, the present calculations give order of range of temperature increases in the core.

ACKNOWLEDGEMENTS

The authors wish to thank CNRS (JACE program) for the financial support of this work in the frame of the PCR program "Thorium Molten Salt Reactor". Daniel Heuer and Sylvie Sanchez are warmly thank for numerous helpful discussions. We also thank Victor Ignatiev for his numerous constructive remarks and help concerning molten salt properties data.

NOMENCLATURE

c_p : heat capacity ($\text{J kg}^{-1} \text{K}^{-1}$)
 d_1 : channel diameter (m)
 d_2 : molten salt+carbon system diameter (m)
 d_h : hydraulic diameter
 δ : boundary layer thickness (m)
 f : friction factor
 g : gravity acceleration (m s^{-2})
 h : convective heat transfer coefficient ($\text{W m}^{-2} \text{K}^{-1}$)

L : length (m)
 μ : dynamic viscosity (Pa)
 N : channel number in the carbon matrix
 Nu : Nusselt number
 p : power density (MW m⁻³)
 P : pressure (Pa)
 Pr : Prandtl number
 q : heat flux (W m⁻²)
 Q : mass flow rate per channel (kg s⁻¹)
 λ : conduction coefficient (W m⁻¹ K⁻¹)
 r : radial coordinate (m)
 Re : Reynolds number
 ρ : density (kg m⁻³)
 S : surface area (m²)
 T : temperature (K)
 ΔT : temperature variation (K)
 τ_p : wall shear stress (Pa)
 V : velocity (m s⁻¹)
 Vol : volume (m³)
 z : axial coordinate (m)

subscript

ms: molten salt
c: carbon
int:interface

REFERENCES

- Alexandre A., *Cours de Modélisation*, 3^{ème} année ENSMA school course
Bayazitoglu Y. and Necati Özişik N. 1988, *Elements of Heat Transfer*, ed. Mc Graw Hill
Dauwson D. and Trass O. 1972, *Int. J. Heat Mass Transfer*. 15, 1317
European Commission. Reactor physics study June 2003, design review and nominal operating conditions, non proliferation issues MOST –D2&3
Fluent[®], Tutorial Guide volumes 1-3, 1998, Fluent Incorporated
Fluent[®], User's Guide volumes 1-4, 1998, Fluent Incorporated
Janssen L.P.B.M. and Warmoeskerken M.M.C.G. 1987, *Transport Phenomena Data Companion*, Ed. Arnold DUM
Moody L.F. 1944, *Trans. Am. Soc. Mech. Eng.* 66, 671
Nayyar M.L. 1992, *Piping Handbook*. Sixth Edition McGraw-Hill
Nuttin A., Heuer D., Billebaud A., Brisot R., Le Brun C., Liatard E., Loiseaux J.M., Mathieu L., Meplan O., Merle-Lucotte E., Nifenecker H., Perdu F. 2005, *Progress in nuclear energy*, 46, 1, p77
Nuttin. A. 2002, *Potentialité du concept de réacteur à sels fondus pour une production durable d'énergie nucléaire basée sur le cycle thorium en spectre épi thermique*, PhD thesis (UJF– Grenoble I)
Patankar S. V. 1980, *Numerical Heat Transfer and Fluid Flow*. Taylor & Francis
Perdu. F. 2003, *Contribution aux études de sûreté pour des filières innovante de réacteurs nucléaires*, PhD thesis (UJF – Grenoble I)
Salvatores M. 2004, *Traitement et gestion des déchets radioactifs : la transmutation*, ENSCP school course
Saulnier J.B., *Cours de Transferts Thermiques*, ENSMA school course
Sisson L.E., Pitts D.R. 1977, *Elements of transport phenomena*. Mc-Graw-Hill Book company
White F.M.1979, *Fluid Mechanics*. Second edition McGraw-Hill